ELSEVIER

Journal of Chromatography A, 680 (1994) 33–42

JOURNAL OF CHROMATOGRAPHY A

The use of a microconcentric column in capillary electrophoresis

Chuzo Fujimoto*, Hirofumi Matsui, Hirokazu Sawada, Kiyokatsu Jinno

Department of Materials Science, Toyohashi University of Technology, Toyohashi 441, Japan

Abstract

The results from preliminary investigations into the use of a concentric column having a thin (*ca.* 95 μm) separation chamber for capillary electrophoresis (CE) are presented. The concentric column is constructed by winding a plastic line helically on a fused-silica capillary and then by inserting it into a larger diameter fused-silica capillary. Characteristics of the concentric column are determined and compared with conventional CE columns. The microconcentric column allows increased sample loading over the conventional columns while maintaining peak integrity. The feasibility of using the concentric column for micropreparative CE is demonstrated by the collection of fractions and subsequent analysis by analytical CE.

1. Introduction

The need for the isolation of small amounts (less than 1 μg) of purified components for use as standards or for characterization, especially in the fields related to biology and medicine, is increasing. There is no doubt that the materials to be examined in the future are present at even smaller levels in extraordinarily complex mixtures or are too labile to be amenable to conventional methods. In response to this challenge, much research has been directed toward the development of preparative techniques based upon capillary electrophoresis (CE).

In CE, the inner diameter (I.D.) of the column is the key to achieve highly efficient separations. Since the emergence of CE in 1981 [1,2], separations in narrow-bore columns (100 μm or less) have been recommended to minimize the effect of Joule heating generated by the passage of electrical current through the separation buffer. With wide-bore capillaries, a significant radial temperature gradient can be formed within the column bore, which in turn results in density gradient and convection. Such convection means sample zone broadening. Because of the high inner surface-area-to-internal volume ratio (the S/V ratio, typically more than several tens mm^{-1}), broadening of sample zones is minimized by effective dissipation of heat through the surrounding walls.

Assuming that sample volumes occupy 1% of the total column volume, the injection volume for a 100 μm I.D. capillary with a 50 cm length will be approximately 40 nl. When the initial concentration of the desired constituent is in the order of mg/ml, the injected amount is 40 ng: this represents 40 pmol to a constituent having a relative molecular mass of 1000. The loading capacity of CE is well above the detection limits

* Corresponding author. Present address: Department of Chemistry, Hamamatsu University School of Medicine, Hamamatsu 431-31, Japan.

0021-9673/94/$07.00
SSDI 0021-9673(94)00282-E

of mass spectrometry (MS) even if the whole mass range is scanned, or even if MS–MS experiments are to be performed [3,4]. Also, automated high-sensitivity methods are capable of the sequence determination of peptide samples at levels of less than 20 pmol [5]. However, as is often the case, further material is necessary to make the identification or sequence of the isolated components more reliable and to enable the purified material to be used as standards.

Provided that the generated heat is rapidly removed from the column, the sample loading capacity of CE should be proportional to the cross-sectional area of the separation column. Smith and co-workers [6,7] investigated the use of larger bore capillaries (150 or 200 μm I.D.). They showed that the larger I.D. capillaries provide a resolution of peptides comparable to that obtained with common analytical capillaries (50 μm I.D. or 75 μm I.D.). Although the starting peptide concentrations were in the mg/ml range, this approach demonstrated sequence analysis at low-pmol levels of peptides.

Tsuda *et al.* [8] demonstrated that increasing the sample load capacity can be achieved by the use of a rectangular cross-section capillary column in stead of a circular cross-section capillary column. Rectangular borosilicate-glass capillaries with dimensions ranging from 195 μm × 16 μm to 1000 μm × 50 μm were employed. Because of the large S/V ratio, and hence the excellent heat dissipation ability, large cross-sectional rectangular capillaries can be used without loss in separation efficiencies.

Other approaches that permit larger sample loading included a multicapillary system [7,9–12], field amplified sample loading [13–15], isotachophoretic sample loading [16–18], and a concentrator capillary system [12,19]. Each method has its own advantages and disadvantages, which have been reviewed previously [20–22].

In this paper, we explore the use of a microconcentric column for micropreparative CE separations. Electrophoresis is carried out in a separation chamber which is formed between coaxially disposed, double fused-silica capillaries. The double capillary column allows much higher sample loading than a single capillary column without degrading peak integrity.

2. Experimental

2.1. Construction of the microconcentric column

The procedure for preparing a microconcentric column is illustrated in Fig. 1. We use commercially available fused-silica tubings (GL Sciences, Tokyo, Japan) to construct the microconcentric column. The inner capillary is a 5-μm I.D. (or 10 μm I.D.) × 375 μm O.D. fused-silica tubing with an external coating. In order to remove the coating, the capillary is immersed in concentrated sulphuric acid at ambient temperature overnight. After this treatment the coating can be readily peeled off. The capillary is thoroughly washed with tap water and deionized water, and is then dried at ambient temperature. The naked capillary has now an O.D. of approximately 340 μm. Next, a line having a nominal diameter of 90 μm is wound around the bare fused-silica

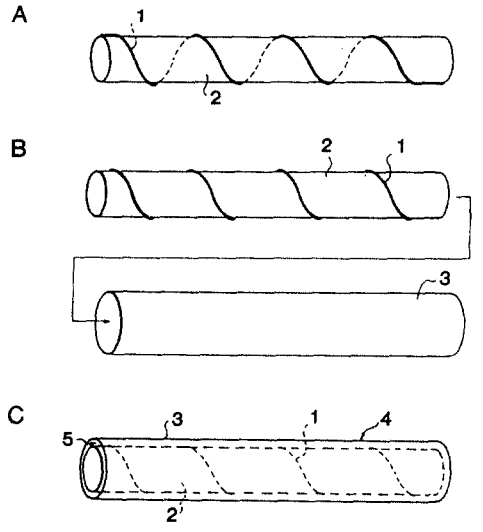

Fig. 1. Steps illustrating the construction of the concentric column. (A) Prepare a clad-removed fused-silica tube, used as the inner tube of the column, and wind a line helically around it; (B) insert the inner tube into a wider I.D. fused-silica tube; (C) completed. 1 = line; 2 = inner tube; 3 = outer tube; 4 = polyimide clad of outer tube; 5 = separation chamber.

capillary (Fig. 1A). A glue is placed on each end of the capillary to fix the line on the capillary. The line is made of synthetic resin and available from several sources (*e.g.*, Toray, Tokyo, Japan). Column construction is easy when the number of turns is 40 to 100 per meter along the column axis. At smaller numbers of turns, the inner capillary is not fixed well in the outer capillary. On the other hand, at larger numbers of turns, it is hard to insert the line-wound, inner capillary into the outer capillary. The line-wound capillary is inserted into a 530 μm I.D. × 630 μm O.D. fused-silica capillary tubing (GL Sciences) with polyimide clad (Figs. 1B and 1C). A detection window is made on the outer capillary by burning off the polyimide with an electrically heated filament before the column is assembled.

2.2. Apparatus

The apparatus used is pictured in Fig. 2. Surprisingly, the microconcentric column is fairly robust once it is assembled. The columns are flexible and can be looped into relatively small diameters (smaller than 18 cm). This permits a U-shape column configuration (Fig. 2B) besides the straight column configuration (Fig. 2A). The former configuration can be advantageous when designing a compact apparatus.

For preparative work, an electrical connector was made on the microconcentric column as described previously [23]. Briefly, a small portion of the polyimide coating is removed from the outer capillary at a distance of 2 cm from the outlet end. After the exposed section is cemented onto a plastic mount, the bared area of the capillary is scratched. A fracture is produced by bending the column carefully at the scratch until it breaks. The fracture is then surrounded by a certain thickness of polyacrylamide gel (10%T–3.6%C). The polyacrylamide joint is placed in a buffer reservoir that is connected to a high voltage. By this means, an extremely higher flow resistance exists in the direction of the fracture so that the bulk flow is directed toward the column outlet [11,23]. The quantity of the sample which may be lost through the fracture should depend on the ratio of the flow resistances in the two directions [11], which will be negligible in this case.

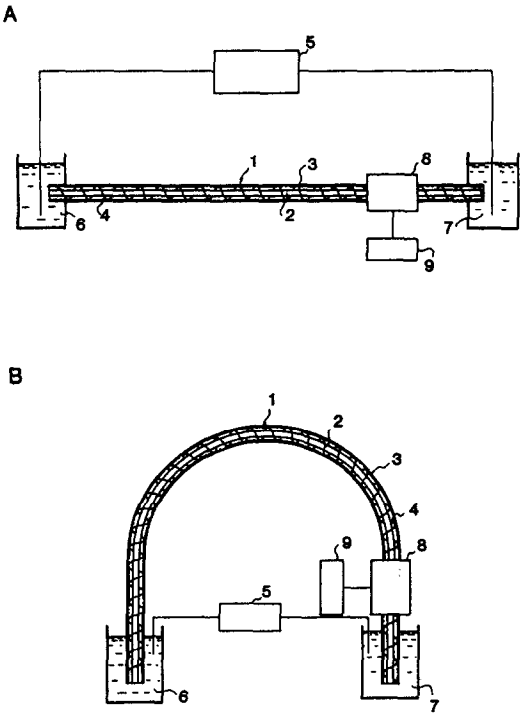

Fig. 2. CE setups with the microconcentric column. (A) Straight column configuration; (B) U-shape column configuration. 1 = Line; 2 = inner tube; 3 = outer tube; 4 = polyimide clad of outer tube; 5 = high-voltage power supply; 6 = inlet-end buffer reservoir; 7 = outlet-end buffer reservoir; 8 = UV detector; 9 = integration system.

On-column detection was accomplished using a modified UV detector (Model 870-CE, Jasco, Tokyo, Japan). The wavelength was set at 220 nm. The microconcentric, double capillary column was attached to a capillary mount which was made in-house for detection. Care was taken to ensure that the coiled line did not intercept the light from the UV source. For experiments using a single capillary column, the commercial capillary amount (Part No. 6627-425A, Jasco) was employed as received. A 50 μm × 500 μm slit (Part No. 6680-4117A, Jasco) was affixed on the backside of these capillary mounts. The signal from the detector was fed to a Labchart 180 (System Instruments, Tokyo, Japan) integration system.

A Matsusada Precision Devices (Kusatsu, Japan) Model HSR-30N-TU negative power supply was used to provide the electrical field for electrophoresis. The current in the system was measured over a 10-kΩ resistance in the return circuit of the power supply by means of a digital multimeter (Model VOAC 81, Iwatsu Electric, Tokyo, Japan). No column temperature control was available.

2.3. Chemicals

Tris(hydroxymethyl)aminomethane (Tris) and 2-[4-(2-hydroxyethyl)-1-piperazinyl]ethanesulfonic acid (HEPES) were obtained from Nacalai Tesque (Kyoto, Japan). All buffers were prepared daily using water from a Milli-Q unit (Millipore, Bedford, MA, USA). The other chemicals were of analytical grade and purchased from various distributors.

2.4. Estimation of sample plug length

The Fanning (or Darcy) equation can be used to estimate the sample plug length introduced into a column due to a pressure difference across the length of the column [24]:

$$\Delta p = 4f(\rho v^2/2g_c)(L/D_h) \quad (1)$$

where Δp is the pressure difference across the column (kgf m^{-2}; kgf = kilogram-force), f is the Fanning friction factor (dimensionless), ρ is the density of the fluid (kg m^{-3}), v is the average velocity of the fluid (m s^{-1}), g_c is dimensional constant (kg m $kgf^{-1}s^{-2}$), L is the length of the column (m), and D_h is the hydraulic (or equivalent) diameter (m). For hydrodynamic (gravity) flows, Δp is given by

$$\Delta p = \rho g\, \Delta h/g_c \quad (2)$$

where g is the constant for gravitation acceleration (m s^{-2}) and Δh is the height difference between the fluid levels at both ends of the column (m). The hydraulic diameter for circular cross-section columns equals to the geometric diameter, D (m), whereas that for concentric annular columns is given by

$$D_h = D_o - D_i \quad (3)$$

where D_o and D_i are the O.D. and I.D. of the annulus, respectively. The Fanning restriction factors are

$$f = 16/Re \text{ (for circular cross section columns)} \quad (4)$$

$$f = 16\{(D_o - D_i)^2/[(D_o^2 + D_i^2) - (D_o^2 - D_i^2)/\ln(D_o/D_i)]\}/Re$$

(for concentric annular columns) (5)

where Re is the Reinolds number (dimensionless) and is defined as

$$Re = \rho v D_h/\eta \quad (6)$$

where η is the Newtonian viscosity of the fluid (kg $m^{-1}s^{-1}$).

Substituting Eqs. 4 and 6 into Eq. 1 gives

$$\Delta p = 32v\eta L/g_c D^2 \quad (7)$$

which is known as the Hagen–Poiseuille equation. The pressure difference for the concentric annular columns is

$$\Delta p = 32v\eta L/\{g_c[(D_o^2 + D_i^2) - (D_o^2 - D_i^2)/\ln(D_o/D_i)]\} \quad (8)$$

The average velocity of the sample introduced by gravity flow at a given height difference for circular cross-section columns and concentric annular columns can be obtained from Eqs. 7 and 8, respectively. Multiplication of the average fluid velocity by the introduction time gives the length of sample introduced during hydrodynamic flow introduction:

$$l = \rho g\, \Delta h\, D^2 t_i/32\eta L \text{ (for circular cross section columns)} \quad (9)$$

$$l = \rho g\, \Delta h\, t_i[(D_o^2 + D_i^2) - (D_o^2 - D_i^2)/\ln(D_o/D_i)]/32\eta L$$

(for concentric annular columns) (10)

where t_i is the introduction time (s).

3. Results and discussion

3.1. Characterization of the microconcentric column

The heat dissipation ability of a CE column should depend upon the S/V ratio while the sample loading ability should depend upon the cross-sectional area of the column. Table 1 summarizes several characteristics of the three types of columns having different dimensions. From the table we can see that the concentric column allows the sample load that is enhanced by a factor of 16.6, although the S/V ratio for the concentric column is about one-half of that for a 100-μm I.D. capillary column. In general, the use of wider bore columns (*e.g.*, 150 μm I.D. columns) is somewhat limited in that a dramatic increase in separation efficiency is observed [8,25]. The sample loading ability of the concentric column is higher by a factor of 2.6 than a 1000 μm × 50 μm rectangular column, although the heat dissipation is expected to be less effective with the former column than with the latter column.

There are further advantages of the concentric column over the rectangular column. Because the concentric column is made of fused-silica, it shows good transparency at short wavelengths (<210 nm) of UV detection, which is perhaps the most widely used CE detection method, unlike the rectangular column which is made of borosilicate glass. This advantage is manifested when short wavelength UV detection is used for detecting proteins and peptides [26–29]. According to Mayer and Miller [30], the absorbance at 193 nm is directly proportional to the number of peptide bonds in the molecule. More importantly, detection at 193 nm yields higher absorbance for peptide bonds [30]. The line of mercury at 185 nm can be also used for detection of peptides and oligosaccharides which are separated by CE with certain buffers [31].

The concentric column also alleviates the problem of the capillary fragility which has been encountered with the borosilicate-glass rectangular columns. Because the concentric column is flexible like a single fused-silica capillary column, it is not necessary to cut a channel in the optical compartment of the UV detector when installing the column to the detection unit (see Ref. [8]). In addition, the flexibility of the concentric column allows the design of a compact apparatus, as mentioned in the Experimental section.

With the use of the concentric column for CE, a question needs to be addressed before the column performance is examined: does the solute go through the helical channel that is formed by partitioning the space between the double capillaries with the line? Note that the calculated space (*ca.* 95 μm) is larger than the nominal diameter of the line. To answer this question, methyl orange was dissolved in water at a high concentration. A 5-mm wide section of the polyimide coating was removed from the outer

Table 1
Characteristics of columns having different separation chamber shapes

Shape of cross section	Circle	Rectangle	Rectangle	Annulus
Materials	Fused-silica	Borosilicate	Borosilicate	Fused-silica
Size, μm	100 I.D.	16 × 195[a]	50 × 1000[a]	340 I.D. × 530 O.D.
Circumference, mm	$3.14 \cdot 10^{-1}$	$4.22 \cdot 10^{-1}$	2.10	2.73
Cross-sectional area, mm^2	$7.85 \cdot 10^{-3}$	$3.12 \cdot 10^{-3}$	$5.00 \cdot 10^{-2}$	$1.30 \cdot 10^{-1}$
Rel. cross-sectional area	1.00	$3.97 \cdot 10^{-1}$	6.37	16.6
S/V, mm^{-1}	40	135	42	21

[a]Values taken from Ref. [8].

capillary (44 cm in length) at a distance of 2 cm from the inlet, and placed on the sample stage of a microscope. The column and the outlet reservoir were filled with 100 m*M* HEPES, pH 5.2, while the inlet reservoir was filled with the dye solution. Each end of the column was placed into the reservoirs and then a high voltage (− 10 kV) was applied over the column. We were able to observe the dye traveling through the helical separation channel under the microscope.

It is worth noting that the separation channel is not very extended by winding the line. For example, the increment in the separation length is estimated to be only *ca.* 0.6% for a 50-cm long column having 50 turns of the line. It follows that the change in the field strength at a given voltage is negligible. The effect of a helical separation channel on the separation efficiency was not examined because of the difficulties in performing such an experiment, although some previous work [32,33] showed that in open tubular columns, no significant effect of column coiling occurred while the influence of coiling on efficiency was significant with gel-filled columns. Alternatively, the influence of using the U-shaped column configuration (Fig. 2B) was investigated, and as a result, it was found that this column configuration did not influence the column performance.

The effects of Joule heating on the separation have been generally a great concern when working with large cross-sectional columns, since increasing the cross-sectional area causes an increase in the electric current passing through the column, which can seriously reduce the efficiency of the system. Because the amount of heat that must be removed is proportional to the square of the field strength, the equivalent conductance and the buffer concentration [34], the choice of these parameters becomes critical when using large bore columns. Low conductivity and low concentration buffers have been used to circumvent the heating problems [6–8], despite the problems of limited sample loading and possible adsorption effects [25]. It was expected that this would be the case for the authors' column system. To investigate the influence of excessive heat generation, the applied field strength *vs.* the resulting current was plotted. The results are shown in Fig. 3 for the four running solutions, which were chosen for having low conductivities. The field strength at which the curve begins to deviate from the linearity can be considered as the maximum voltage, beyond which the generated heat is excessive for the column system [35,36]. In the present work, the maximum field strength for each running solution was tentatively defined as the value beyond that the correlation coefficient begins to drop below 0.998 on the linear regression analysis. The results are shown in Table 2, together with the values of the heat generation rate. It can be seen that the maximum field strength and the heat generation rate per meter for the concentric column are in the same order of magnitude as is common for CE separations using circular cross-section capillaries without any cooling system (see, Ref. [37]). On the other hand, because of the increased volume of the concentric column, the heat generation rate per unit volume is two orders of magnitude smaller than that for circular cross-section capillaries operated under typical conditions (see, Ref. [34]). Undoubtedly, Good's buffers are the most promising candidates for such a large cross-sectional column, since they can cover a wide range of pH while

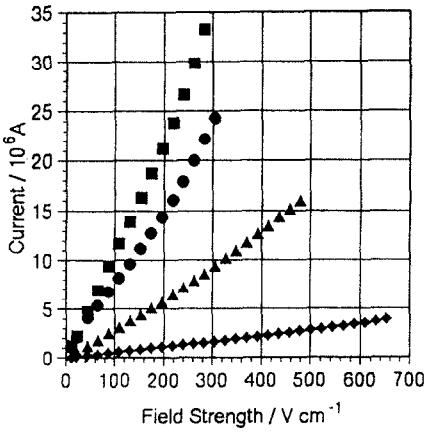

Fig. 3. Plots of applied field strength *vs.* resulting current for different running solutions. ■ = 5 m*M* HEPES, pH 7.0; ● = 100 m*M* HEPES, pH 5.2; ▲ = 3 m*M* Tris, pH 9.2; ◆ = 5 m*M* HEPES, pH 5.2. Column length, 46 cm.

Table 2
The heat generation rate at the maximum field strength

Buffer medium	Maximum field strength ($V\ cm^{-1}$)	Heat generation rate ($W\ m^{-1}$)	($W\ cm^{-3}$)
3 m*M* Tris, pH 9.2	413	0.558	4.29
5 m*M* HEPES, pH 7.0	260	0.777	5.98
5 m*M* HEPES, pH 5.2	630	0.213	1.79
100 m*M* HEPES, pH 5.2	260	0.467	3.59

having low conductivities even at high concentrations.

To evaluate whether or not concentric annular columns maintain CE performance, a mixture containing dansyl acid (0.05 mg/ml) and benzyl alcohol (1.0 mg/ml) was electrophoresed with a concentric annular column and circular cross-section capillary columns (100 and 250 μm I.D.). The sample was introduced by the gravity flow for 6 s at 5 cm and then a voltage of −10 kV was applied. Note that the lengths of the sample introduced into individual columns are not equal (see Experimental section for the estimation of the sample plug length). A comparison of the electropherograms obtained with those columns is shown in Fig. 4. A summary of the migration time, peak width, peak asymmetry and plate count for the benzyl alcohol peak is given in Table 3. With either the concentric column or the 100-μm I.D. capillary column, the components eluted with base line resolution; the peaks are only partially resolved with the 250-μm I.D. capillary column. It is worthy to note that *the volumes* introduced into the 250-μm I.D. column and the concentric column are almost the same, being 40 times that of the 100-μm I.D. column: the volumes of sample applied to the former columns are approximately 0.73 μl and the amounts of dansyl acid and benzyl alcohol are 36 ng and 730 ng, respectively. The migration times of the components are longer with the concentric column than with the 100-μm I.D. capillary column, indicating that the rate of electroosmotic flow is smaller with the concentric column compared with the 100-μm I.D. circular cross-section capillary. This would be responsible for the difference in the state of the inner surface between those columns. We can also see that the concentric column and the 100-μm I.D. column are different in the values of plate count and resolution. There are several probable explanations for this. First, in this case, the decrease in the velocity of electroosmotic flow can yield improved resolution and a decrease in plate count. Second, the concentric column was operated near the maximum field strength for the buffer, which makes the heat dissipation less effective. Third, the injection length of the

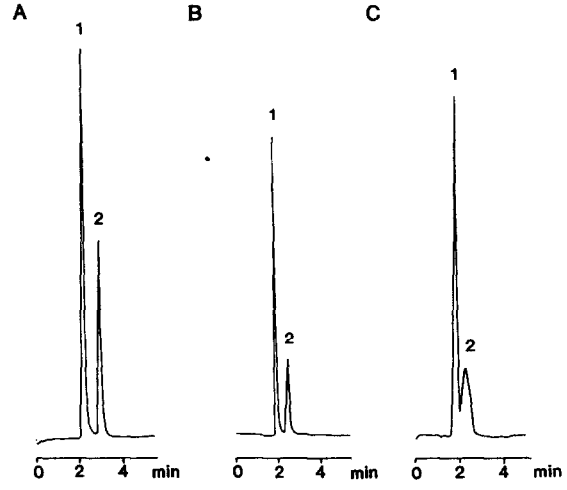

Fig. 4. Electropherograms of benzyl alcohol and dansyl acid for microconcentric column (A) and round cross-section columns of 100 μm I.D. (B) and 250 μm I.D. (C). Peaks: 1 = benzyl alcohol; 2 = dansyl alcohol. Conditions: 46 cm column length (27 cm effective column length) each; −10 kV applied voltage; 220 nm detection wavelength; 3 m*M* Tris buffer, adjusted to pH 9.2 with glycine.

Table 3
Summary of column performance determination experiments

Column	100 μm I.D.	250 μm I.D.	Concentric
Migration time, min	1.87	1.84	2.18
Peak width[a], s	5.2	10.6	8.6
Peak asymmetry[b]	2.82	1.07	1.66
Plate count[c], m^{-1}	5606	1306	2786
Resolution[d]	1.29	N.D.[e]	2.79

Conditions as in Fig. 4. Average values are given for benzyl alcohol ($n = 5$).
[a] Based on half height peak width measurement.
[b] Based on 15% peak height.
[c] Calculated using the equation: $N = 5.54(t/w_h)^2$; where t is the migration time of the peak and w_h is the half-height peak width.
[d] Resolution between benzyl alcohol (peak 1) and dansyl acid (peak 2) was determined by the equation: $R = (t_2 - t_1)/(w_{1R} + w_{2L})$; where t_1 and t_2 are the migration times of peaks 1 and 2 ($t_2 > t_1$), w_{1R} is the portion of the width of peak 1 which is to the right of t_1, and w_{2L} is the portion of the width of peak 2 which is to the left of t_2.
[e] Not determined.

sample for the concentric column is longer by a factor of 2.4 than that for the 100-μm I.D. capillary. The two latter matters tend to decrease the efficiency of separation. It follows that direct comparison of the column performance between those columns is inappropriate. However, it seems to us that the separation power is adequate for many applications and can be improved by optimizing the operating conditions.

Table 4 shows the relative standard deviation (R.S.D.) in the migration time and peak area for the concentric column, together with those for the 100-μm I.D. capillary column. From the table we can see that the values obtained with the concentric column are comparable to those for the 100-μm I.D. column.

3.2. Eluate collection

The concentric column enabled us to collect enough material from a single run. To collect eluate continuously, the electrical circuit in the column was completed prior to its outlet by the use of the polyacrylamide joint. This design allows the collection of fractions at an electrically isolated outlet [11,23]. Thymine was dissolved at a concentration of 1.0 m*M* in a 100-m*M* HEPES (pH 5.2) buffer and injected into the concentric column having a polyacrylamide joint with gravity flow for 6 s at 5 cm. The resulting electropherogram is shown in Fig. 5A. The amount of sample applied is approximately 92 ng. We can see a thymine peak eluting at 5.95 min from the electropherogram. Eluate was collected into a

Table 4
Comparison of R.S.D. values of the concentric column system and the circular column system ($n = 5$)

Component	Concentric		100 μm I.D.	
	Migration time	Peak area	Migration time	Peak area
Benzyl alcohol	0.461	5.83	1.56	5.51
Dansyl acid	1.87	6.95	1.65	4.67

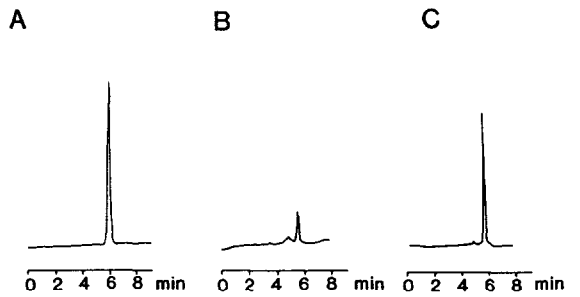

Fig. 5. (A) Electropherogram of thymine on microconcentric column; (B) electropherogram of fraction collected from preparative run, obtained on 100 μm I.D. analytical column; (C) electropherogram of thymine on 100 μm I.D. analytical column. Conditions: 46 cm column length (27 cm effective column length) each; −10 kV applied voltage; 220 nm detection wavelength; 100 m*M* HEPES buffer, pH 5.2. The polyacrylamide joint (on-column fracture) is positioned 2 cm from the exit of the concentric column. The lengths of the columns over which the high voltage is applied are 44 cm and 46 cm in (A) and (B), respectively.

small vial during the period 1.5–3.5 min after the emergence of the thymine peak on the UV electropherogram. The UV detector was located 10 cm prior to the column outlet and the time required for the analyte to travel from the detection point to the column outlet was approximately 98 s. Electrophoresis of the collected fraction (*ca.* 16 μl in volume) was carried out using a second CE system with a 100-μm I.D. circular capillary column. A small portion (*ca.* 8.3 nl) of the fraction was syphoned for 12 s at 5 cm. The resulting electropherogram is shown in Fig. 5B, where the thymine peak appears at 5.47 min and an artificial peak appears at 4.85 min. Because the migration times of thymine were different for the two columns, we injected the original sample solution into the 100-μm I.D. column. As expected, the peak of thymine was observed to elute at the same migration time as that of the collected fraction (see Fig. 5C). This indicates that the concentric column can be employed for micropreparative purposes. A comparison between the electropherograms in Figs. 5A and C reveals that the peak width is broader with the concentric column than with the 100-μm I.D. column: the calculated plate counts were 7320 m^{-1} and 22 790 m^{-1} for the concentric column and the 100-μm I.D. column, respectively. Further work is required for the explanation for the lower plate count with the concentric column, but it seems to us that the decreased velocity of electroosmotic flow and the lengthened sample plug are in part responsible for the difference in plate count.

4. Conclusions

We have demonstrated that large quantities of separated components could be continuously collected from a single separation using a concentric column. The column provides many favorable features, involving ease of construction, robustness and UV transparency at short wavelengths. Obviously, more work is required to fully evaluate microconcentric columns for use as preparative columns. These include the optimization of the O.D. of the inner tube and the I.D. of the outer tube, the proper selection of the buffer for the particular separation, the use of a cooling system and the development of an injection system that is suited for the concentric column. We expect further improvement in the column performance when these conditions are realized.

Acknowledgements

This work was supported partly by the Asahi Glass Foundation, the Nakano Foundation and the Research Foundation of Toyohashi University of Technology.

References

[1] J.W. Jorgenson and K.D. Lukas, *Anal. Chem.*, 53 (1981) 1298.
[2] J.W. Jorgenson and K.D. Lukas, *J. Chromatogr.*, 218 (1981) 209.
[3] C. Schwer and F. Lottspeich, *J. Chromatogr.*, 623 (1992) 345.
[4] R. Takagiku, T. Kough, M.P. Lacey and R.E. Schneider, *Rapid Commun. Mass Spectrosc.*, 4 (1990) 24.

[5] B.L. Karger, A.S. Cohen and A. Guttman, *J. Chromatogr.*, 492 (1989) 585.
[6] A. Smith and J.W. Kenny, *Tech. Protein Chem.*, 3 (1991) 113.
[7] J.W. Kenny, J.I. Ohms and A. Smith, *Tech. Protein Chem.*, 4 (1992) 363.
[8] T. Tsuda, J.V. Sweedler and R.N. Zare, *Anal. Chem.*, 62 (1990) 2149.
[9] N.A. Guzman, L. Hernandez and B.G. Hoebel, *BioPharm.*, 2 (1989) 22.
[10] T. Hanai, H. Hatano, N. Nimura and T. Kinoshita, *J. High Resolut. Chromatogr.*, 13 (1990) 573.
[11] C. Fujimoto, Y. Muramatsu, M. Suzuki and K. Jinno, *J. High Resolut. Chromatogr.*, 14 (1991) 178.
[12] N.A. Guzman, M.A. Trebilcock and J.P. Advis, *J. Liquid Chromatogr.*, 14 (1991) 997.
[13] D.S. Burgi and R.L. Chien, *Anal. Chem.*, 63 (1991) 2042.
[14] R.L. Chien and D.S. Burgi, *J. Chromatogr.*, 559 (1991) 141.
[15] R.L. Chien and D.S. Burgi, *J. Chromatogr.*, 559 (1991) 153.
[16] F.E.P. Mikkers, F.M. Everaerts and Th.P.E.M. Verheggen, *J. Chromatogr.*, 169 (1979) 1.
[17] P. Jandik and W.R. Jones, *J. Chromatogr.*, 546 (1991) 431.
[18] S. Hjerten, K. Elenbring, F. Kilar, J.-L. Liao, A.J.C. Chen, C.J. Siebert and M.-D. Zhu, *J. Chromatogr.*, 403 (1987) 47.
[19] M.E. Swartz and M. Merion, *J. Chromatogr.*, 632 (1993) 209.
[20] T. Tsuda, in N.A. Guzman (Editor), *Capillary Electrophoresis Technology*, Marcel Dekker, New York, 1993, Ch. 14, p. 489.
[21] C. Fujimoto and K. Jinno, in N.A. Guzman (Editor), *Capillary Electrophoresis Technology*, Marcel Dekker, New York, 1993, Ch. 15, p. 509.
[22] F. Foret, L. Krivankova and P. Bocek, *Capillary Zone Electrophoresis*, VCH, Weinheim, 1993, Ch. 8, p. 187.
[23] C. Fujimoto, T. Fujikawa and K. Jinno, *J. High Resolut. Chromatogr.*, 15 (1992) 201.
[24] R.H. Perry (Editor), *Chemical Engineer's Handbook*, McGraw-Hill Kogakusha, Tokyo, 5th ed., 1976, Section 5.
[25] R.J. Nelson, A. Paulus, A.S. Cohen, A. Guttman and B.L. Karger, *J. Chromatogr.*, 480 (1989) 111.
[26] J. Tehrani, R. Macomber and L. Day, *J. High Resolut. Chromatogr.*, 14 (1991) 10.
[27] R.M. McCormic, *Anal. Chem.*, 60 (1988) 2322.
[28] J.J. Kirkland and R.M. McCormic, *Chromatographia*, 24 (187) 58.
[29] J.S. Green and J.W. Jorgenson, *J. Chromatogr.*, 478 (1989) 63.
[30] M.M. Mayer and J.A. Miller, *Anal. Biochem.*, 36 (1970) 91.
[31] M. Fuchs, P. Timmoney and M. Merion, presented at *HPCE'91, San Diego, CA, 1991*, Poster No. PM/24.
[32] S. Wicar, M. Vilenchik, A. Belenkii, A.S. Cohen and B.L. Karger, *J. Microcol. Sep.*, 4 (1992) 339.
[33] T. Srichaiyo and S. Hjerten, *J. Chromatogr.*, 604 (1992) 85.
[34] J. Knox, *Chromatographia*, 26 (1988) 329.
[35] R. Kuhn and S. Hoffstetter-Kuhn, *Capillary Electrophoresis: Principles and Practice*, Springer-Verlag, Berlin, 1993, Ch. 3, p. 37.
[36] F. Foret, L. Krivankova and P. Bocek, *Capillary Zone Electrophoresis*, VCH, Weinheim, 1993, Ch. 4, p. 37.
[37] M.J. Sepanik and R.O. Cole, *Anal. Chem.*, 59 (1987) 472.